

ITVTON: Virtual Try-On Diffusion Transformer Based on Integrated Image and Text

Haifeng Ni
East China Normal University
Shanghai, China
haifengni99@gmail.com

Ming Xu
East China Normal University
Shanghai, China
mxu@cs.ecnu.edu.cn

Faming Fang
East China Normal University
Shanghai, China
fmfang@cs.ecnu.edu.cn

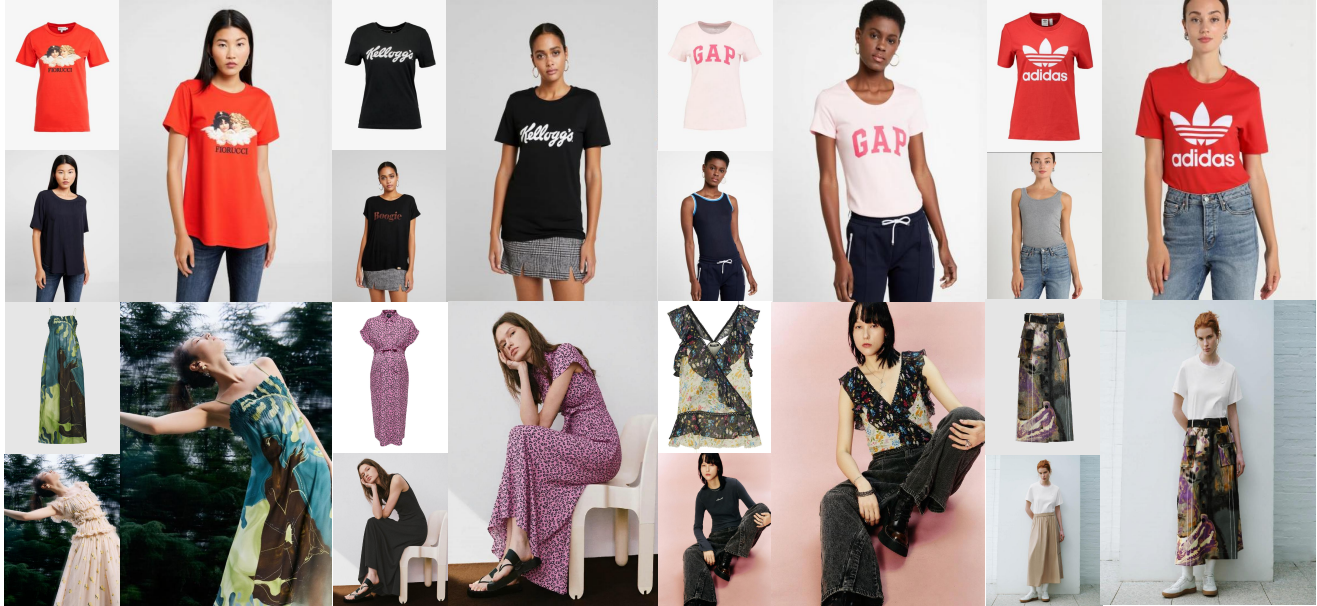


Figure 1. The ITVTON model is utilized to create virtual try-on images derived from the VITON-HD [4] dataset (first row) and the filtered IGPair [25] dataset (second row). For optimal visual evaluation, it is recommended to examine the images in their enlarged form.

Abstract

Virtual try-on, which aims to seamlessly fit garments onto person images, has recently seen significant progress with diffusion-based models. However, existing methods commonly resort to duplicated backbones or additional image encoders to extract garment features, which increases computational overhead and network complexity. In this paper, we propose ITVTON, an efficient framework that leverages the Diffusion Transformer (DiT) as its single generator to improve image fidelity. By concatenating garment and person images along the width dimension and incorporating textual descriptions from both, ITVTON effectively captures garment-person interactions while preserving realism. To further reduce computational cost, we restrict training to the attention parameters within a single Diffusion Transformer (Single-DiT) block. Extensive experiments demon-

strate that ITVTON surpasses baseline methods both qualitatively and quantitatively, setting a new standard for virtual try-on. Moreover, experiments on 10,257 image pairs from IGPair confirm its robustness in real-world scenarios.

1. Introduction

Virtual try-on technology [3, 7, 9] has emerged as an indispensable tool in e-commerce and personal fashion, significantly enhancing consumers' shopping experiences by generating realistic try-on images and offering novel marketing avenues for brands and retailers. Traditional methods often rely on Generative Adversarial Networks (GANs) [10] in a two-stage process: first warping the garment according to the person's pose, then using a generator to merge the warped garment with the person image. Although these

approaches improve image realism, they heavily depend on the warping module, leading to potential overfitting, unstable generation quality, limited generalization, and difficulties in handling complex backgrounds or dynamic poses.

Recently, diffusion models [26, 27] have emerged as a compelling alternative for virtual try-on tasks, owing to their superior generative capabilities and enhanced flexibility. Unlike GAN-based pipelines, diffusion models [23, 24] tend to generate more stable, high-quality, and diverse outputs. They also possess strong control and optimization properties during training, making them well-suited for addressing challenges in virtual try-on. Current diffusion-based virtual try-on methods primarily adopt parallel U-shaped UNet structures [22], typically introducing a garment UNet alongside a generative UNet, with attention mechanisms bridging garment features and the person image. While this approach substantially advances virtual try-on, it also entails additional network modules and higher computational costs at both training and inference stages.

Building upon the progress in diffusion transformers (DiT) [18], our goal is to harness their scalability and generative performance to improve virtual try-on image quality. To streamline the network design and jointly capture person and garment information, we avoid auxiliary image encoders by instead concatenating the garment and person images along the width dimension. As the DiT model capitalizes on textual cues, we further enhance realism by introducing textual descriptions of both the garment and person. Within the transformer backbone, image and text signals are fused directly through attention mechanisms, which proves critical for improving garment-person interactions. To reduce computational overhead, we focus training solely on the attention parameters within a single DiT block (Single-DiT), thereby striking a balance between performance and efficiency.

Contributions.

- We propose *ITVTON*, a DiT-based virtual try-on model that leverages the strong scaling and generative capabilities of DiT to preserve fine-grained garment features and enhance interactions with person images.
- We align try-on results by concatenating garment and person images along the width dimension, integrating image-text descriptions for improved generation quality. This design eliminates the need for an extra image encoder, resulting in a compact network structure.
- We introduce a parameter-efficient training scheme that targets only the attention parameters within a Single-DiT block, reducing training time and computational overhead while enhancing stability and output fidelity.

2. Related Work

The virtual try-on task [9] involves generating a realistic photograph of a model wearing a specified outfit while

maintaining consistency in other regions. Scholars initially explored generative adversarial networks (GANs)[10] for this task, employing a two-stage process: aligning the garment with the model and fusing them via a GAN-based network. VITON-HD[4] introduces ALignment-Aware Segment (ALIAS) normalization to address misalignment by segmenting and fitting garments. GP-VTON [31] proposes a Local-Flow Global-Parsing (LFGP) warping module and a dynamic gradient truncation strategy to simulate garment deformation more effectively. However, GAN-based models suffer from unstable training and struggle to preserve garment texture details.

Recently, diffusion models have demonstrated superior stability and quality in virtual try-on. LADI-VTON [17] and DCI-VTON [11] align garments with the body before using diffusion models for fusion. TryOnDiffusion [35] employs a parallel UNet to unify garment deformation and fusion. OOTDiffusion [32] captures detailed clothing features in a single step, while IDM-VTON [5] incorporates the IP-Adapter and pose guidance for enhanced control. Paint-by-Example [33] reframes try-on as an inpainting problem, fine-tuning diffusion models on virtual try-on datasets to enable fine-grained image control.

Much work has been inspired by the PCDMs [24] second-stage inpainting conditional diffusion model, which uses the concatenation of source conditions and target images and is gradually gaining popularity in virtual try-on tasks. For example, CatVTON [6] similarly fine-tunes the restoration diffusion model but eliminates the text encoder and cross-attention block, training only the self-attention block to create a lightweight network structure. IC-LoRA [14] posits that the text-to-image diffusion transformer model [18] is inherently contextually generative, enabling high-quality image generation through integrated captioning of multiple images using small datasets (e.g., 20–100 samples) with task-specific LoRA [13] tuning. In this paper, we adopt the DiT model as a prior and achieve a high-quality, high-fidelity virtual try-on task through a simple network architecture and an efficient training strategy, which involves splicing garment and person images along the width dimension and using integrated image-text descriptions as inputs. Additionally, our approach further improves generation performance and training efficiency while maintaining a lightweight network structure.

3. Proposed Method

3.1. Background on Diffusion Model

Stable Diffusion. The stable diffusion [21] is a prominent example of the latent diffusion model. It comprises a variational autoencoder (VAE) \mathcal{E}_θ , a CLIP [19] text encoder τ_θ , and a denoising UNet ϵ_θ . The key advantage is that image information is compressed into a low-dimensional la-

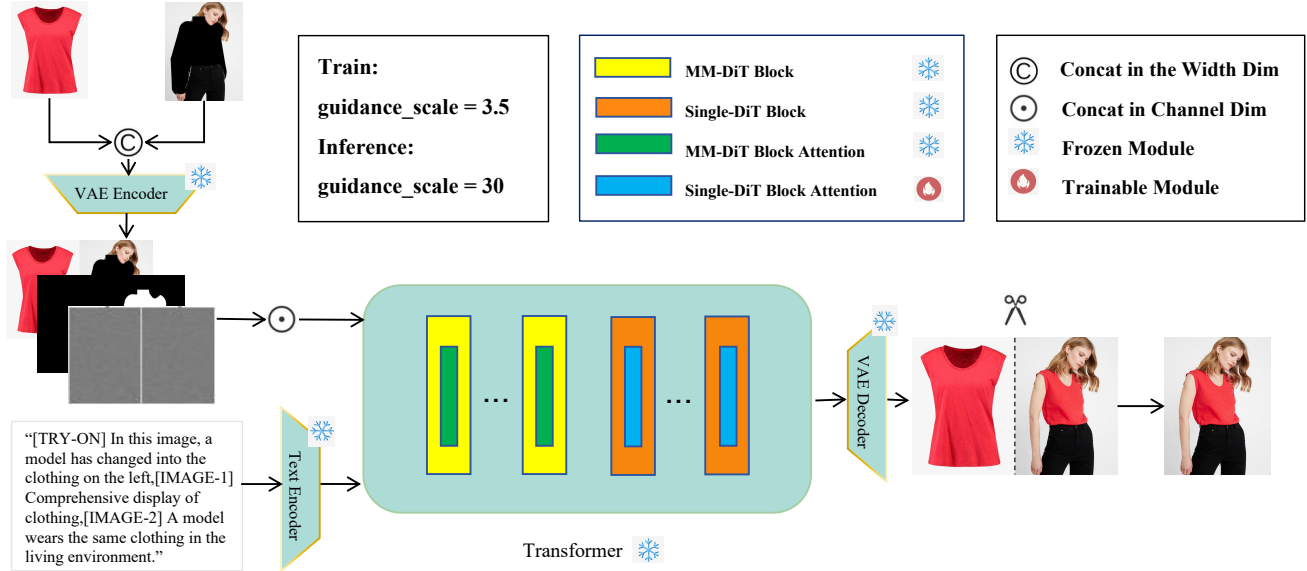


Figure 2. Overview of ITVTON. Our approach achieves high-quality virtual try-on by concatenating the garment image with the target person image along the width dimension and incorporating integrated image-text representations (as illustrated in the figure). Only the attention parameters in the Single-DiT module remain learnable during training, ensuring a streamlined and efficient try-on network.

tent space, which significantly reduces the computational cost associated with training and inference. The input consists of an image \mathbf{x} along with textual cues \mathbf{y} , and the following loss function is minimized during training:

$$\mathcal{L}_{LDM} = \mathbb{E}_{\mathcal{E}_{\theta}(\mathbf{x}), \mathbf{y}, \epsilon \sim \mathcal{N}(0,1), \mathbf{t}} [\|\epsilon - \epsilon_{\theta}(\mathbf{Z}_{\mathbf{t}}, \mathbf{t}, \tau_{\theta}(\mathbf{y}))\|_2^2], \quad (1)$$

where $\mathbf{t} \in \{1, \dots, T\}$ represents the time step of forward noise addition in the diffusion model, and $\mathbf{Z}_{\mathbf{t}}$ denotes the VAE-encoded image with added random noise $\epsilon \sim \mathcal{N}(0, 1)$.

FLUX. FLUX is a type of diffusion model that employs the DiT architecture and is trained using a parameterized rectified flow model (RF) [8]. The training process of FLUX is defined as a rectified flow that links the data distribution to the noise distribution via a straight line. A key characteristic of the forward process is that $\mathbf{z}_{\mathbf{t}}$ is obtained by linearly interpolating the data \mathbf{x}_0 and the noise ϵ , i.e.:

$$\mathbf{z}_{\mathbf{t}} = (1 - \mathbf{t})\mathbf{x}_0 + \mathbf{t}\epsilon, \epsilon \sim \mathcal{N}(0, 1), \quad (2)$$

The core concept of the rectified flow technique employed in FLUX is to streamline the training and inference processes by introducing a flow-matching method that enhances the efficiency of image generation. The loss function is defined as follows:

$$\mathcal{L}_{RF} = -\frac{1}{2} \mathbb{E}_{\mathbf{t} \sim \mathcal{U}(\mathbf{t}), \epsilon \sim \mathcal{N}(0,1)} [\mathbf{w}_{\mathbf{t}} \lambda_{\mathbf{t}} \|\epsilon_{\Theta}(\mathbf{z}_{\mathbf{t}}, \mathbf{t}) - \epsilon\|^2], \quad (3)$$

where $\lambda_{\mathbf{t}}$ corresponds to a signal-to-noise ratio and $\mathbf{w}_{\mathbf{t}}$ is a time dependent-weighting factor. $\epsilon_{\Theta}(\mathbf{z}_{\mathbf{t}}, \mathbf{t})$ denotes the network parameters of the transformer module.

3.2. ITVTON

The ITVTON architecture, illustrated in Figure 2, aims to generate high-quality and high-fidelity virtual try-on images using a simple network structure and minimal training cost. This section outlines the components of our network architecture and the underlying architectural rationale, as well as explores efficient parameter training strategies.

3.2.1. Network Module

Previous approaches primarily focus on achieving detailed alignment between garments and persons. For instance, LADI-VTON [17] first warps the garments to match the model’s pose, then uses a diffusion model to blend the warped garments with the model. IDM-VTON [5] employs a parallel UNet to extract garment features and incorporates an attention mechanism into the generative UNet to maintain alignment during virtual try-on. However, these methods either lack sufficient accuracy or necessitate the introduction of additional network modules for their implementation, failing to meet our expectations.

We found that the mature generative model exhibits a strong ability to generate masked regions; for example, when the mouth of a face is masked, the model is likely to generate an intact face upon repair. Based on this, if the clothing area of the model is masked and subsequently fed into the model along with a garment image and a mask image, what would happen during repair? The model would likely generate content for the masked area based on the image information outside the mask. However, to generate a

high-quality and high-fidelity image of the garment change, the model must also be trained and fine-tuned. Furthermore, because the attention mechanism of FLUX’s transformer module processes image information in conjunction with textual data, it is beneficial to leverage the model’s textual input.

Consequently, we directly incorporate the three modules:

VAE: The VAE encoder transforms pixel-level images into a latent representation to optimize computational efficiency. Compared to traditional VAEs, the FLUX series VAE outputs latent features. Before these features are fed into the diffusion model, a patching operation is performed, stacking 2×2 pixel blocks directly along the channel dimension. This method preserves the original resolution of each pixel block and prevents the loss of critical image feature information. Consequently, we concatenate the garment and person features along the width dimension, leveraging the robust capabilities of the VAE while ensuring alignment between inputs.

Text Encoder: Two text encoders (CLIP ViT-L and T5-XXL [20]) process textual prompts as input, enabling the generation of more controllable, high-quality images. Inspired by IC-LoRA [14], multi-image integrated text inputs have a positive impact on virtual try-on tasks. Therefore, we utilize multi-image integrated text (text format shown in Figure 2) as input, enhancing the controllability and quality of the generated images.

Transformer: The transformer synthesizes the final try-on image by integrating features from the latent space. It accepts concatenated garment and person features, along with noise and masks as image inputs, and receives multi-image integrated titles as text inputs. By seamlessly integrating all this information, the transformer facilitates effective learning and synthesis of the final try-on image.

Our network architecture does not rely on additional modules, and the try-on task can be efficiently performed using only the inherent functionality of the model.

3.2.2. Architectural Inference

In this work, we utilize stitched garment and person images as input and employ integrated image-text pairs as the textual input. This approach ensures a streamlined network architecture and simplifies the preprocessing steps prior to inference.

Specifically, consider a garment image $\mathbf{I}_g \in \mathbb{R}^{3 \times H \times W}$ and a person image $\mathbf{I}_p \in \mathbb{R}^{3 \times H \times W}$, which are concatenated along the width dimension to generate $\mathbf{C}_{gp} \in \mathbb{R}^{3 \times H \times 2W}$. The corresponding binary, clothing-agnostic mask map of the person image, denoted $\mathbf{m}_p \in \mathbb{R}^{H \times W}$, is concatenated with an all-zero mask map of the same dimensions to produce $\mathbf{m}_{op} \in \mathbb{R}^{H \times 2W}$.

$$\mathbf{C}_{gp} = \mathbf{I}_g \odot \mathbf{I}_p, \quad (4)$$

$$\mathbf{m}_{op} = \mathbf{O} \odot \mathbf{m}_p, \quad (5)$$

where \odot denotes concatenation along the width dimension, \mathbf{O} represents an all-zero mask image. \mathbf{C}_{gp} is multiplied with the processed elements of \mathbf{m}_{op} to generate the clothing-agnostic person and garment-spliced image $\mathbf{C}_{masked} \in \mathbb{R}^{3 \times H \times 2W}$. \mathbf{C}_{masked} is then encoded using the VAE encoder \mathcal{E} to obtain $\mathbf{V}_{masked} \in \mathbb{R}^{16 \times \frac{H}{8} \times \frac{2W}{8}}$, which has a channel value of 16. Finally, \mathbf{m}_{op} is interpolated to produce $\mathbf{X}_{om} \in \mathbb{R}^{64 \times \frac{H}{8} \times \frac{2W}{8}}$ with a channel value of 64.

$$\mathbf{C}_{masked} = \mathbf{C}_{gp} \otimes (1 - \mathbf{m}_{op}), \quad (6)$$

$$\mathbf{V}_{masked} = \mathcal{E}(\mathbf{C}_{masked}), \quad (7)$$

where \otimes is used for element-wise multiplication. \mathbf{V}_{masked} and \mathbf{X}_{om} undergo a packing operation to generate $\mathbf{P}_{masked} \in \mathbb{R}^{64 \times (\frac{H}{8 \times 2} \times \frac{2W}{8 \times 2})}$ and $\mathbf{P}_{om} \in \mathbb{R}^{256 \times (\frac{H}{8 \times 2} \times \frac{2W}{8 \times 2})}$, respectively, before being fed into the transformer module. The channel values are scaled by a factor of 4, while the width and height are each halved, then multiplied and compressed into a single-dimensional value.

$$\mathbf{P}_{masked} = \text{pack}(\mathbf{V}_{masked}), \quad (8)$$

$$\mathbf{P}_{om} = \text{pack}(\mathbf{X}_{om}), \quad (9)$$

The text encoder τ processes the integrated image-text pair, producing τ_{text} . Prior to noise reduction, \mathbf{P}_{masked} and \mathbf{P}_{om} are concatenated along the channel dimension with random noise \mathbf{Z}_t of the same size as \mathbf{P}_{masked} , which is then fed into the transformer module to predict \mathbf{Z}_{t-1} alongside τ_{text} .

$$\mathbf{Z}_{t-1} = \text{Transformer}(\mathbf{Z}_t \odot \mathbf{P}_{masked} \odot \mathbf{P}_{om}, \tau_{text}), \quad (10)$$

where \odot denotes the splicing operation along the width dimension. $\mathbf{Z}_0 \in \mathbb{R}^{64 \times (\frac{H}{8 \times 2} \times \frac{2W}{8 \times 2})}$ is obtained after t -steps of cyclic noise reduction, followed by $\mathbf{V}_{con} \in \mathbb{R}^{16 \times \frac{H}{8} \times \frac{2W}{8}}$, which is generated after the unpacking operation. Next, $\mathbf{I}_{con} \in \mathbb{R}^{3 \times H \times 2W}$ is derived through VAE decoding. The final image $\mathbf{I}_{result} \in \mathbb{R}^{3 \times H \times W}$ is produced after cropping.

3.2.3. Parameter-Efficient Training

The pre-trained DiT model demonstrates strong capability and robustness in generating masked regions; however, fine-tuning is required to ensure accurate interaction between garment and person features, thereby generating efficient images. On the other hand, these pre-trained models already possess a wealth of prior knowledge, and an excessive number of trainable parameters not only increases the training burden—requiring more GPU memory and a longer training duration—but may also degrade the model’s existing performance.

The Transformer in FLUX comprises the MM-DiT block structures and the Single-DiT block structures. The MM-DiT block facilitates the fusion of the two modal information streams, which are subsequently fed into the Single-DiT block to deepen the model’s architecture and enhance

its learning capability. Additionally, a parallel attention mechanism is incorporated into the Single-DiT blocks to further optimize model performance. The attention within these blocks fuses both image and text information for processing. We hypothesized that the attention mechanism is crucial for achieving high-quality results and conducted experiments to identify the most relevant blocks. Specifically, we configured the trainable components as the all attention layer, the attention layer in the MM-DiT block, and the attention layer in the Single-DiT block. The experimental results indicate that training all attention layers, the attention layer in the MM-DiT block, and the attention layer in the Single-DiT block can generate satisfactory trial-wear effects; however, the metrics obtained by training the attention layer in the Single-DiT block are optimal, with the lowest number of training parameters. Therefore, we employ a parameter-efficient training strategy to fine-tune the attention layer within the Single-DiT block, which contains 1076.2M parameters. Additionally, we apply a 10% probability to discard multi-image integrated text cues during training to improve the model’s generalization ability.

4. Experimentation and Analysis

4.1. Datasets

Our experiments utilized two publicly available fashion datasets: VITON-HD [4] and IGPair [25]. The VITON-HD [4] dataset comprises 13,679 image pairs, including 11,647 pairs in the training set and 2,032 pairs in the test set. Each pair consists of a frontal upper-body image of a person paired with an upper-body clothing image, both at a resolution of 768×1024 . The IGPair [25] dataset contains 324,857 image pairs with clothing classified into 18 categories encompassing a broad spectrum of styles, such as casual, formal, sports, fashion, and vintage. For each apparel item, 2 to 5 model images taken from various angles are provided, with a resolution of 1024×1280 . From these, we meticulously selected 10,381 image pairs featuring the same model in multiple poses while wearing the same attire. Of these pairs, 10,257 are allocated for training purposes, with the remainder reserved for testing. We employ OpenPose [2, 28, 30] and HumanParsing [16] to generate garment-independent masks and uniformly adjust the resolution of all images to 768×1024 pixels.

4.2. Implementation Details

We utilize the pre-trained FLUX.1-Fill-dev model for training. We trained the model on the VITON-HD [4] dataset and evaluated its performance against other approaches using a designated test set. Additionally, we trained the model on the IGPair [25] dataset to assess its generative capability in realistic scenarios. Each model was trained with identical hyperparameters: 36,000 steps at a resolution of 384×512

Methods	<i>SSIM</i> \uparrow	<i>FID</i> \downarrow	<i>KID</i> \downarrow	<i>LPIPS</i> \downarrow
DCI-VTON [11]	0.8620	9.408	4.547	0.0606
StableVITON [15]	0.8543	6.439	0.942	0.0905
GP-VTON [31]	0.8701	8.726	3.944	0.0585
OOTDiffusion [32]	0.8187	9.305	4.086	0.0876
IDM-VTON [5]	0.8499	5.762	0.732	0.0603
CatVTON [6]	0.8704	5.425	0.411	0.0565
ITVTON (Ours)	0.8734	5.064	0.264	0.0530

Table 1. Quantitative Comparison with Other Methods. We compare metric performance in paired settings on the VITON-HD [4] dataset. The best and second-best results are bolded and underlined, respectively.

using the AdamW 8-bit optimizer, a batch size of 4, and a constant learning rate of $1e-5$. All experiments were conducted on a single NVIDIA A100 GPU.

4.3. Qualitative Comparison

We evaluated the visual quality using the VITON-HD [4] dataset. As shown in Figure 3, it demonstrates the try-on effects of various styles and patterns from the dataset, and compares the try-on variations across different methods. While other methods encounter issues such as color discrepancies and inconsistent details during virtual try-ons, ITVTON delivers more realistic and detailed outcomes owing to its simplicity and efficiency.

Additionally, we assess ITVTON on selected IGPair [25] datasets and benchmark it against other diffusion-based VTON methods. As shown in Figure 4, ITVTON demonstrates its capability to accurately recognize and model the shape of complex garments, such as a sheath dress, and seamlessly integrate them with human figures. Notably, it can generate high-quality images even in complex poses (e.g., sitting on the chair). In intricate field scenes, ITVTON effectively handles the integration of backgrounds with clothing, maintaining consistency and realism across diverse and challenging environments.

4.4. Quantitative Comparison

For the inference results of the test pair dataset, we use two metrics, frechet inception distance (FID) [12] and kernel inception distance (KID) [1], to compare the gap between real and generated images, and two metrics, structural similarity index (SSIM) [29] and learned perceptual image patch similarity (LPIPS) [34] which are two metrics to measure the overall structural and perceptual similarity between images.

We conducted a quantitative evaluation of several state-of-the-art open-source virtual try-on methods using the VITON-HD [4] dataset. Comparisons were made in paired settings to assess the similarity between the synthesized results and ground truth, as well as the model’s generalization performance. The results, presented in Table 1, show

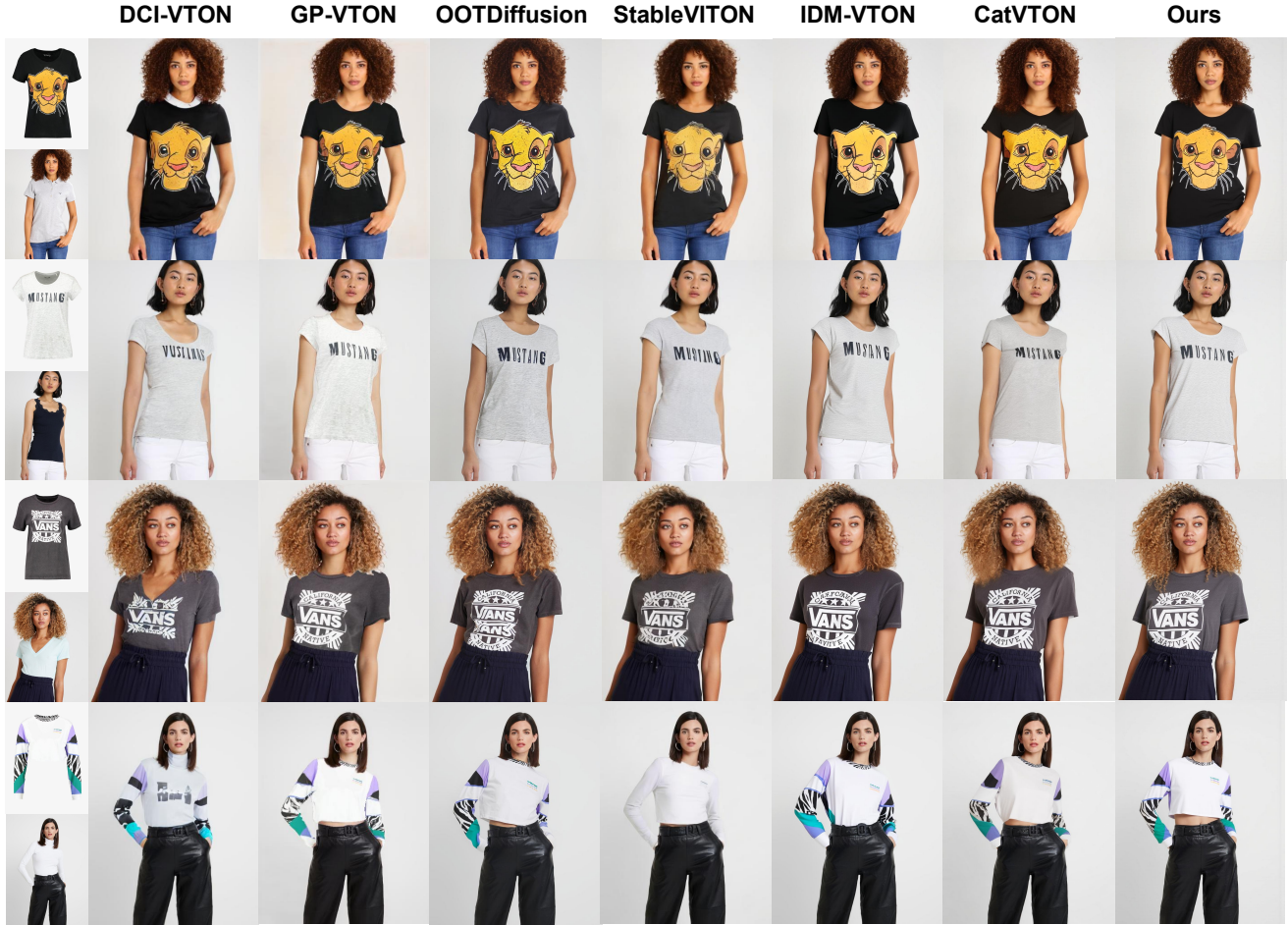


Figure 3. Qualitative comparison on the VITON-HD [4] Dataset. ITVTON exhibits significant advantages in processing complex patterns and text. We recommend zooming in for a detailed inspection.

that our method outperforms all others across all metrics. This demonstrates the efficacy of our simplified network architecture and parameter fine-tuning in virtual try-on tasks. Additionally, the data indicates that both CatVTON [6] and IDM-VTON [5] demonstrated strong performance in virtual try-on tasks.

4.5. Ablation Studies

We conducted an ablation study to investigate the effects of several factors:

1. different trainable modules,
2. the inclusion or exclusion of multi-image integrated text during both training and inference,
3. the impact of the guidance scale on the try-on results.

For a fair comparison, we trained different versions of the model using the VITON-HD [4] dataset.

Trainable Modules: As shown in Figure 5, we evaluated three trainable modules in Transformer: 1) all attention pa-

rameters. 2) attention parameters of MM-DiT blocks. 3) attention parameters of Single-DiT blocks, with progressively fewer trainable parameters. Table 2 presents the evaluation results on the VITON-HD [4] dataset. We observe that the model trained with attention parameters within the Single-DiT block performs optimally across three metrics. The other metric, KID, shows only a slight decrease compared to the model that trains all attention parameters, while the Single-DiT model uses only 1076.2M attention parameters. Fewer training weights both reduce memory requirements and speed up training, and do not pull down performance. This demonstrates that training the attention parameters within the Single-DiT block is optimal.

Multi-Image Integrated Text: Ordinary text, such as “A model is wearing a top.” and multi-image integrated text are illustrated in Figure 2. Both types of text inputs were employed during training and inference. As shown in Table 3, two metrics (SSIM and LPIPS) perform optimally

Trainable Module	$SSIM \uparrow$	$FID \downarrow$	$KID \downarrow$	$LPIPS \downarrow$	Trainable Params(M)
All Attention	0.8702	5.155	0.250	0.0557	1611.23
MM-DiT Block Attention	0.8641	5.438	0.332	0.0578	1434.93
Single-DiT Block Attention	0.8734	5.064	0.264	0.0530	1076.2

Table 2. Ablation results of different trainable module on VITON-HD [4] dataset. Taken together, the results indicate that training the attention parameters within the Single-DiT block achieves the optimal performance. The best results are shown in bold.

Train		Inference		$SSIM \uparrow$	$FID \downarrow$	$KID \downarrow$	$LPIPS \downarrow$
Ordinary Text	Integrated Text	Ordinary Text	Integrated Text				
✓	-	✓	-	0.8727	5.178	0.377	0.0534
✓	-	-	✓	0.8737	5.169	0.379	0.0529
-	✓	✓	-	0.8723	5.098	0.298	0.0537
-	✓	-	✓	0.8734	5.064	0.264	0.0530

Table 3. Ablation results from post-training inference on the VITON-HD [4] dataset using different text inputs are presented. The best results are shown in bold. Overall, training with integrated text and reasoning with integrated text yield the best performance.

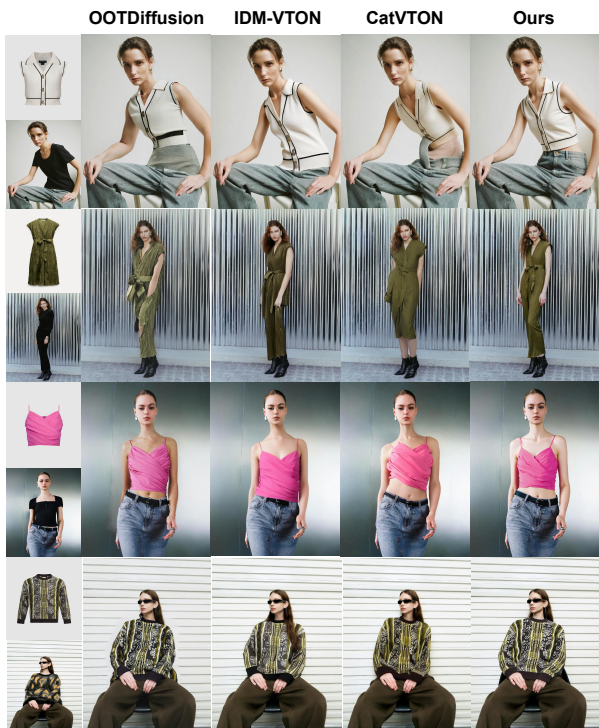


Figure 4. Qualitative comparison in field scenarios demonstrates that our method generates more natural try-on effects, even in complex scenes and with varied postures.

when only multi-image integrated text is used during inference, although the improvement is marginal compared to the model using multi-image integrated text for both training and inference. Additionally, the other two metrics (FID

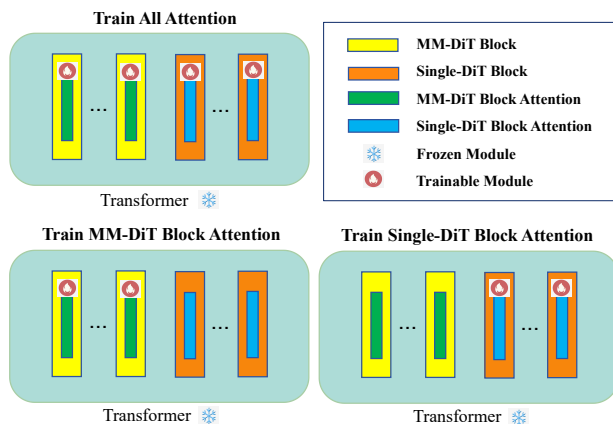


Figure 5. Train the different modules in the Transformer.

Guidance_Scale	$SSIM \uparrow$	$FID \downarrow$	$KID \downarrow$	$LPIPS \downarrow$
2	0.8727	5.246	0.394	0.0532
3.5	0.8734	5.064	0.264	0.0530
30	0.8748	5.068	0.267	0.0540

Table 4. Ablation results for various guidance scale settings during training. The best results are shown in bold. Setting the guidance scale to 30 during inference and to 2, 3.5, and 30 during training results in very similar values for the four metrics of the VITON-HD [4] test set. However, collectively, a guidance scale of 3.5 emerges as the optimal setting.

and KID) are optimal for the model that utilizes multi-image integrated text for both training and inference, demonstrating that this approach is the most effective.



Figure 6. Comparison of the effects of setting different guidance scales during training. The model with the guidance scale set to 30 during inference and the guidance scale set to 2 or 30 during training does not perform well when generating garments with text or complex patterns. In contrast, the model with the guidance scale set to 3.5 during training performs well.

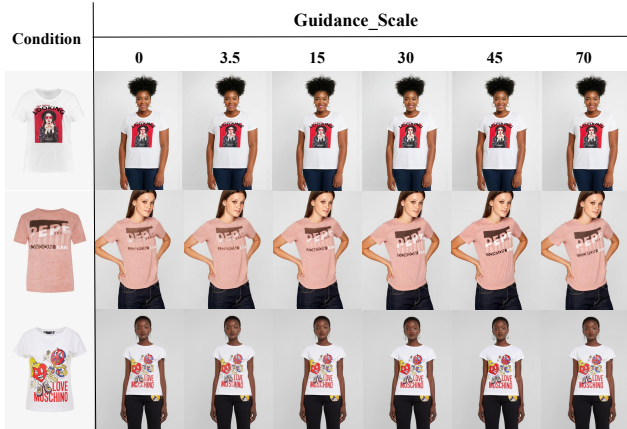


Figure 7. Comparison of the effects of setting different guidance scales during inference. Setting the guidance scale to 3.5 for training and 30 or 45 for inference yields the best performance. If set to other values, issues such as color discrepancies and pattern disruption may occur.

Guidance Scale: The guidance scale is crucial in both the training and inference processes of the FLUX model. First, adjust the guidance scale setting to 30 for inference, as shown in Table 4. The metrics FID, KID, and LPIPS achieve optimal results with a guidance scale setting of 3.5

during training, while the SSIM metric is slightly lower compared to the model with a guidance scale of 30 during training. This suggests that setting the guidance scale to 3.5 during training yields better performance. As shown in Figure 6, models with the guidance scale set to 2 or 30 during training do not perform well when generating garments with repeated or intricate patterns, while models with the guidance scale set to 3.5 can accurately reproduce repeated patterns or images. Next, set the guidance scale to 3.5 for training and evaluate the effects of different guidance scale settings during inference. As shown in Figure 7, setting the guidance scale to 30 or 45 during inference results in the best restoration of color and pattern. For example, setting the guidance scale to 0 during inference results in color discrepancies and broken patterns. In summary, setting the guidance scale to 3.5 for training and 30 for inference yields the best inference results.

4.6. Constraints and Social Impacts

Although our model yields high-quality try-on results, it has certain limitations. The accuracy of the try-on process is highly dependent on the precision of the input mask; inaccurate masking can significantly degrade the quality of the generated output. For instance, if the mask fails to fully cover the person’s garment, the try-on results will be adversely affected by exposed areas of the garment. Additionally, character features such as hairstyles, jewelry, muscle contours, and tattoos within the masked area may undergo alteration during the generation process. These limitations underscore the necessity for precise preprocessing and further refinement of the model to ensure the consistency and reliability of the output.

From a societal perspective, ITVTON can help users to effectively visualize themselves in a particular outfit, and therefore our approach must be used responsibly, requiring users to be careful to protect image ownership from malicious manipulation, such as unethically modifying personal images.

5. Conclusion

In this paper, we introduced ITVTON, a simple yet effective virtual try-on diffusion transformer model with 1,076.2M trainable parameters. ITVTON spliced garment and person images along the width dimension, taken integrated image-text descriptions as input, and required only fine-tuning to generate high-quality, high-fidelity virtual try-on images. Extensive experiments have demonstrated that ITVTON could achieve superior qualitative and quantitative results compared to state-of-the-art methods, while maintaining a simple and efficient network architecture. These findings also suggested that ITVTON would hold significant potential for widespread application in virtual try-on technology.

References

- [1] Mikołaj Bińkowski, Danica J. Sutherland, Michael Arbel, and Arthur Gretton. Demystifying mmd gans, 2021. 5
- [2] Zhe Cao, Tomas Simon, Shih-En Wei, and Yaser Sheikh. Realtime multi-person 2d pose estimation using part affinity fields. In *Proceedings of the IEEE Conference on Computer Vision and Pattern Recognition (CVPR)*, 2017. 5
- [3] Chieh-Yun Chen, Yi-Chung Chen, Hong-Han Shuai, and Wen-Huang Cheng. Size does matter: Size-aware virtual try-on via clothing-oriented transformation try-on network. In *Proceedings of the IEEE/CVF International Conference on Computer Vision (ICCV)*, pages 7513–7522, 2023. 1
- [4] Seunghwan Choi, Sunghyun Park, Minsoo Lee, and Jaegul Choo. Viton-hd: High-resolution virtual try-on via misalignment-aware normalization. In *Proceedings of the IEEE/CVF Conference on Computer Vision and Pattern Recognition (CVPR)*, pages 14131–14140, 2021. 1, 2, 5, 6, 7
- [5] Yisol Choi, Sangkyung Kwak, Kyungmin Lee, Hyungwon Choi, and Jinwoo Shin. Improving diffusion models for authentic virtual try-on in the wild, 2024. 2, 3, 5, 6
- [6] Zheng Chong, Xiao Dong, Haoxiang Li, Shiyue Zhang, Wenqing Zhang, Xujie Zhang, Hanqing Zhao, and Xiaodan Liang. Catvton: Concatenation is all you need for virtual try-on with diffusion models, 2024. 2, 5, 6
- [7] Haoye Dong, Xiaodan Liang, Xiaohui Shen, Bochao Wang, Hanjiang Lai, Jia Zhu, Zhiting Hu, and Jian Yin. Towards multi-pose guided virtual try-on network. In *Proceedings of the IEEE/CVF International Conference on Computer Vision (ICCV)*, 2019. 1
- [8] Patrick Esser, Sumith Kulal, Andreas Blattmann, Rahim Entezari, Jonas Müller, Harry Saini, Yam Levi, Dominik Lorenz, Axel Sauer, Frederic Boesel, Dustin Podell, Tim Dockhorn, Zion English, and Robin Rombach. Scaling rectified flow transformers for high-resolution image synthesis. In *Forty-first International Conference on Machine Learning*, 2024. 3
- [9] Bo Gao, Junchi Ren, Fei Shen, Mengwan Wei, and Zijun Huang. Exploring warping-guided features via adaptive latent diffusion model for virtual try-on. In *2024 IEEE International Conference on Multimedia and Expo (ICME)*, pages 1–6. IEEE, 2024. 1, 2
- [10] Ian Goodfellow, Jean Pouget-Abadie, Mehdi Mirza, Bing Xu, David Warde-Farley, Sherjil Ozair, Aaron Courville, and Yoshua Bengio. Generative adversarial networks. *Commun. ACM*, 63(11):139–144, 2020. 1, 2
- [11] Junhong Gou, Siyu Sun, Jianfu Zhang, Jianlou Si, Chen Qian, and Liqing Zhang. Taming the power of diffusion models for high-quality virtual try-on with appearance flow. In *Proceedings of the 31st ACM International Conference on Multimedia*, page 7599–7607, New York, NY, USA, 2023. Association for Computing Machinery. 2, 5
- [12] Martin Heusel, Hubert Ramsauer, Thomas Unterthiner, Bernhard Nessler, and Sepp Hochreiter. Gans trained by a two time-scale update rule converge to a local nash equilibrium. In *Advances in Neural Information Processing Systems*. Curran Associates, Inc., 2017. 5
- [13] Edward J. Hu, Yelong Shen, Phillip Wallis, Zeyuan Allen-Zhu, Yuanzhi Li, Shean Wang, Lu Wang, and Weizhu Chen. Lora: Low-rank adaptation of large language models, 2021. 2
- [14] Lianghua Huang, Wei Wang, Zhi-Fan Wu, Yupeng Shi, Huanzhang Dou, Chen Liang, Yutong Feng, Yu Liu, and Jingren Zhou. In-context lora for diffusion transformers, 2024. 2, 4
- [15] Jeongho Kim, Guojung Gu, Minho Park, Sunghyun Park, and Jaegul Choo. Stableviton: Learning semantic correspondence with latent diffusion model for virtual try-on. In *Proceedings of the IEEE/CVF Conference on Computer Vision and Pattern Recognition (CVPR)*, pages 8176–8185, 2024. 5
- [16] Peike Li, Yunqiu Xu, Yunchao Wei, and Yi Yang. Self-correction for human parsing. *IEEE Transactions on Pattern Analysis and Machine Intelligence*, 44(6):3260–3271, 2022. 5
- [17] Davide Morelli, Alberto Baldrati, Giuseppe Cartella, Marcella Cornia, Marco Bertini, and Rita Cucchiara. Ladi-vton: Latent diffusion textual-inversion enhanced virtual try-on. In *Proceedings of the 31st ACM International Conference on Multimedia*, page 8580–8589, New York, NY, USA, 2023. Association for Computing Machinery. 2, 3
- [18] William Peebles and Saining Xie. Scalable diffusion models with transformers. In *Proceedings of the IEEE/CVF International Conference on Computer Vision (ICCV)*, pages 4195–4205, 2023. 2
- [19] Alec Radford, Jong Wook Kim, Chris Hallacy, Aditya Ramesh, Gabriel Goh, Sandhini Agarwal, Girish Sastry, Amanda Askell, Pamela Mishkin, Jack Clark, Gretchen Krueger, and Ilya Sutskever. Learning transferable visual models from natural language supervision. In *Proceedings of the 38th International Conference on Machine Learning*, pages 8748–8763. PMLR, 2021. 2
- [20] Colin Raffel, Noam Shazeer, Adam Roberts, Katherine Lee, Sharan Narang, Michael Matena, Yanqi Zhou, Wei Li, and Peter J. Liu. Exploring the limits of transfer learning with a unified text-to-text transformer. *Journal of Machine Learning Research*, 21(140):1–67, 2020. 4
- [21] Robin Rombach, Andreas Blattmann, Dominik Lorenz, Patrick Esser, and Björn Ommer. High-resolution image synthesis with latent diffusion models. In *Proceedings of the IEEE/CVF Conference on Computer Vision and Pattern Recognition (CVPR)*, pages 10684–10695, 2022. 2
- [22] Olaf Ronneberger, Philipp Fischer, and Thomas Brox. U-net: Convolutional networks for biomedical image segmentation. In *Medical Image Computing and Computer-Assisted Intervention – MICCAI 2015*, pages 234–241, Cham, 2015. Springer International Publishing. 2
- [23] Fei Shen and Jinhui Tang. Imagpose: A unified conditional framework for pose-guided person generation. In *The Thirty-eighth Annual Conference on Neural Information Processing Systems*, 2024. 2
- [24] Fei Shen, Hu Ye, Jun Zhang, Cong Wang, Xiao Han, and Wei Yang. Advancing pose-guided image synthesis with progressive conditional diffusion models. *arXiv preprint arXiv:2310.06313*, 2023. 2

- [25] Fei Shen, Xin Jiang, Xin He, Hu Ye, Cong Wang, Xiaoyu Du, Zechao Li, and Jinhui Tang. Imagdressing-v1: Customizable virtual dressing, 2024. [1](#), [5](#)
- [26] Fei Shen, Hu Ye, Sibao Liu, Jun Zhang, Cong Wang, Xiao Han, and Wei Yang. Boosting consistency in story visualization with rich-contextual conditional diffusion models. *arXiv preprint arXiv:2407.02482*, 2024. [2](#)
- [27] Fei Shen, Cong Wang, Junyao Gao, Qin Guo, Jisheng Dang, Jinhui Tang, and Tat-Seng Chua. Long-term talkingface generation via motion-prior conditional diffusion model. *arXiv preprint arXiv:2502.09533*, 2025. [2](#)
- [28] Tomas Simon, Hanbyul Joo, Iain Matthews, and Yaser Sheikh. Hand keypoint detection in single images using multiview bootstrapping. In *Proceedings of the IEEE Conference on Computer Vision and Pattern Recognition (CVPR)*, 2017. [5](#)
- [29] Zhou Wang, A.C. Bovik, H.R. Sheikh, and E.P. Simoncelli. Image quality assessment: from error visibility to structural similarity. *IEEE Transactions on Image Processing*, 13(4): 600–612, 2004. [5](#)
- [30] Shih-En Wei, Varun Ramakrishna, Takeo Kanade, and Yaser Sheikh. Convolutional pose machines. In *Proceedings of the IEEE Conference on Computer Vision and Pattern Recognition (CVPR)*, 2016. [5](#)
- [31] Zhenyu Xie, Zaiyu Huang, Xin Dong, Fuwei Zhao, Haoye Dong, Xijin Zhang, Feida Zhu, and Xiaodan Liang. Gp-vton: Towards general purpose virtual try-on via collaborative local-flow global-parsing learning, 2023. [2](#), [5](#)
- [32] Yuhao Xu, Tao Gu, Weifeng Chen, and Chengcai Chen. Oot-diffusion: Outfitting fusion based latent diffusion for controllable virtual try-on, 2024. [2](#), [5](#)
- [33] Binxin Yang, Shuyang Gu, Bo Zhang, Ting Zhang, Xuejin Chen, Xiaoyan Sun, Dong Chen, and Fang Wen. Paint by example: Exemplar-based image editing with diffusion models. In *Proceedings of the IEEE/CVF Conference on Computer Vision and Pattern Recognition (CVPR)*, pages 18381–18391, 2023. [2](#)
- [34] Richard Zhang, Phillip Isola, Alexei A. Efros, Eli Shechtman, and Oliver Wang. The unreasonable effectiveness of deep features as a perceptual metric. In *Proceedings of the IEEE Conference on Computer Vision and Pattern Recognition (CVPR)*, 2018. [5](#)
- [35] Luyang Zhu, Dawei Yang, Tyler Zhu, Fitsum Reda, William Chan, Chitwan Saharia, Mohammad Norouzi, and Ira Kemelmacher-Shlizerman. Tryondiffusion: A tale of two unets. In *Proceedings of the IEEE/CVF Conference on Computer Vision and Pattern Recognition (CVPR)*, pages 4606–4615, 2023. [2](#)